Journal of Solid Mechanics Vol. 4, No. 1 (2012) pp. 48-58

Effect of Electric Potential Distribution on Electromechanical Behavior of a Piezoelectrically Sandwiched Micro-Beam

A. Shah-Mohammadi-Azar, G. Rezazadeh*, R. Shabani

Mechanical Engineering Department, Urmia University, Urmia, Iran

Received 15 November 2011; accepted 13 January 2012

ABSTRACT

The paper deals with the mechanical behavior of a micro-beam bonded with two piezoelectric layers. The micro-beam is suspended over a fixed substrate and undergoes the both piezoelectric and electrostatic actuation. The piezoelectric layers are poled through the thickness and equipped with surface electrodes. The equation governing the micro-beam deflection under electrostatic pressure is derived according to Euler-Bernoulli beam theory and considering the voltage applied to the piezoelectric layers and Maxwell's equations for the two dimensional electric potential distribution. The obtained nonlinear equation solved by step by step linearization method and Galerkin weighted residual method. The effects of the electric potential distribution and the ratio of the piezoelectric layer thickness respect to the elastic layer thickness on the mechanical behavior of the micro-beam are investigated. The obtained results are compared with the results of a model in which electric potential distribution is not considered.

Keywords: MEMS; Electric potential; Piezoelectric layer; Piezoelectric actuation; Electrostatic actuation

1 INTRODUCTION

NOWADAYS, capacitive based micro-structures like micro-switches, micro-accelerometer, micro-phone and micro-pump are becoming more interesting. In Micro electro-mechanical systems (MEMS) structures, capacitors act as both sensor and actuator. Capacitive sensors, high sensitivity have been proved, and also their stabilities reliabilities [1] have been considered. Recent progresses in micro-machining technology have made production of low cost and reliable micro capacitors possible. There are some challenges with Nano and Micro scaled electromechanical structures, one of them is high driving voltage in RF-MEMS switches, in use applications of wireless system like mobile phones [2], where available DC supply voltages are limited to 3-5 V, while results show driven voltage for used beam in RF-MEMS switch is about 25V, that is unavailable. Some of the achieved efforts to decrease pull-in voltage are like decreasing the gap between substrate and moving plate [3], decreasing the spring constant of the beams [4-5]. Measurement of the surface stress distribution for design reliability assessment is another challenge. Residual stress may cause detrimental effects like buckling of compressive stress, crack of tensile stress [6]. Although compressive or tensile stresses, that are respectively softening and hardening structure stiffness, may be attended as useful from other point of view [7]. Researchers have suggested different methods to measure structure residual stresses. Residual stresses measurement include mechanic, diffraction, ultrasonic a magnetic method [8-9]. Residual stress also affects the microstructure of materials; for example, the developed diffraction strategy from pseudo-grazing incident X-ray diffraction [10], surface stress effect on mechanical behavior in, Nano-

* Corresponding author. Tel.: +98 9141451407.
E-mail address: g.rezazadeh@urmia.ac.ir (G.Rezazadeh).

scaled thin film [11–12] and in Nano-composite [13] solids or structures have been studied. Furthermore, fabrication sequence of actuators and mismatch of both thermal expansion coefficient and crystal lattice period between substrate and thin film in surface micromachining techniques are the examples of the residual stress in MEMS structures. As it is clear, controlling and decreasing these restrictive effects may help designers to have high accuracy in their designs.

Recently, some piezoelectric materials as smart materials play key role in intelligent and modern mechanical, aerospace and civil devices. Piezoelectric materials due to electromechanical interaction properties are considered to be used widely as sensors or actuators. Piezoelectric sensors are mostly made of polymers, PVDF – piezoelectric vinylidene fluoride [10], to make complex geometric shapes produce possible. Mostly ceramics, PZT – piezoelectric zircon ate titan ate lead, due to their high stiffness are used for actuators production. Piezoelectric sensors and actuators importance in active vibration control of the elastic structures [14] are not ignorable. Piezoelectric bonded or embedded sensors and actuators are widely becoming in use, in the MEMS structures. Piezoelectric sensors are used to measure the stiffness of the material [15], as a pressure and temperature sensor [16] or as force sensor [17]. Researchers have attended piezoelectric materials to be used in capacitive based micro-scale sensors and actuators structures. Using of piezoelectric actuation to control the pull-in voltage of a fixed–fixed and cantilever MEM actuators [18], investigation of the natural frequency and the deflection of a micro-beam subjected to combined electrostatic and piezoelectric actuations [19], studying the electromechanical behavior of a micro-beams subjected to piezoelectric and electrostatic actuations [20], studying of static and dynamic stabilities of a micro-beam actuated by a piezoelectric voltage [21], studying of Parametric excitation of a piezoelectrically actuated system near Hopf bifurcation [22].

Therefore, in this paper the suggested method by Rezazadeh et al. [18] for pull-in voltage controlling in electrostatic MEM actuators and estimating residual stress is developed. In the current model, unlike the suggested model by Rezazadeh et al. [18], in which the electric potential distribution is considered one dimensional and linear across the piezoelectric layer thickness, here the electric potential distribution is considered two dimensional as a combination of a half-cosine and linear in the transverse direction and variable along the micro-beam length. In fact the novelty of this paper is considering the effect of the induced electric potential through the piezoelectric layer due to electromechanical interaction effects or piezoelectric direct effects. In this study the micro-beam deflection is modeled based on Euler-Bernoulli beam theory, and the electric potential distribution is modeled based on satisfying the electrostatic Maxwell's equations [23]. The effect of voltages applied to the two bonded upper and lower piezoelectric layers on the micro-beam stiffness and consequently on the pull-in voltage are investigated and compared with those obtained using one dimensional electric potential distribution.

2 MODELING AND FORMULATION

As shown in Fig.1 a clamped-clamped Micro-beam (MEM actuator), bonded with piezoelectric layers from the upper and lower sides, is considered. The micro-beam is with length L, thickness h, width b, gap from the fixed substrate g_o, piezoelectric layers with thickness h_p, with electrostatic actuation voltage V and piezoelectric actuation voltage V_p.

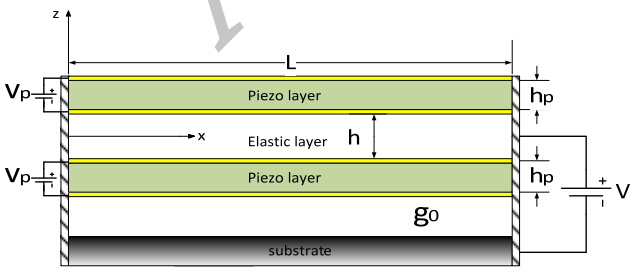

Fig.1
Schematic of clamped-clamped MEM actuator with piezoelectric layers.

To derive governing equations of the problem, based on the Euler-Bernoulli Beam theory, longitudinal displacement, strain and stress of the beam are defined as [18]:

$$u_x(x) = -z\frac{dw}{dx}\ ;\varepsilon_x = -z\frac{\partial^2 w}{\partial x^2};\sigma_x = -Ez\frac{\partial^2 w}{\partial x^2}\ ;w(x,t) = w(x,z,t) \tag{1}$$

where w is the deflection of the beam, and $I = bh^3/12$ is the moment of inertia. E is the elastic layer modulus of elasticity, where for a wide beam, where $b \geq 5h$, the effective modulus of elasticity can approximated by plate modulus ($\tilde{E} = E/\left(1-\upsilon^2\right)$). According to constitutive Eqs. (2) and (3) of a piezoelectric material, mechanical stress strain, respectively σ and ε relation with electric field E and electric displacement D are defined as following [24]:

$$\{\sigma\} = [C]\{\varepsilon\} - [e]^T\{E\} \tag{2}$$

$$\{D\} = [e]\{\varepsilon\} + \left[\varepsilon^{\varepsilon}\right]\{E\} \tag{3}$$

where e is the matrix of piezoelectric coefficient factor, $\varepsilon^{\varepsilon}$ is the component of the dielectric coefficient factor matrix and C is the matrix of modulus of elasticity. In the case of the beam with x directed stress where the length of the beam is significantly larger than its thickness and width, σ_y, σ_z and all shear stresses can be assumed to be zero. So Eq. (2) and Eq.(3) will be reduced into Eq. (4) and Eq. (5). In deed in this case the mechanical stress in terms of mechanical strain and electrical field as indirect effect of piezoelectric effect can be written as Eq. (4) and the electric displacement D_3 along the piezoelectric layer thickness in terms of the mechanical strain and electrical field as the direct of piezoelectric effect can be expressed as Eq. (5) as following [24]:

$$\sigma_x = c_{11,2-D}\varepsilon_x - e_{31,2-D}E_3 \tag{4}$$

$$D_3 = e_{31,2-D}\varepsilon_x + \varepsilon^{\varepsilon}_{3,2-D}E_3 \tag{5}$$

where $c_{11,2-D}$, $e_{31,2-D}$ and $\varepsilon^{\varepsilon}_{3,2-D}$ are the material modified coefficients, and they for plane stress state are obtained as [25]:

$$c_{11,2-D} = c_{11} - \frac{{c_{13}}^2}{c_{33}} \tag{6}$$

$$e_{31,2-D} = e_{31} - e_{33}\frac{c_{13}}{c_{33}} \tag{7}$$

$$\varepsilon^{\varepsilon}_{3,2-D} = \varepsilon^{\varepsilon}_3 + \frac{{e_{33}}^2}{c_{33}} \tag{8}$$

The electric potential distribution in the piezoelectric layer's proposed in the form suggested by Quek and Wang [23], as the combination of a half-cosine and linear variation as following:

$$\phi(x,z,t) = -\cos\left(\frac{\pi z_1}{h_p}\right)\phi_p(x,t) + \frac{z_1}{h_p}\phi_a(t) \tag{9}$$

where z_1 is the local coordinate measured from the center of the piezoelectric layer center. The first term of Eq. (9) shows direct piezoelectric layer effect, famed as eigen potential, induced due to mechanical strain of the beam, and $\phi_a(t) = -V_p$ is the external applied potential difference along the piezoelectric layer thickness. The relation between the electric field and electric potential along the z direction is obtained as [26]:

$$E_3 = -\frac{\pi}{h_p}\sin\left(\frac{\pi z_1}{h_p}\right)\phi_p - \frac{\phi_a(t)}{h_p} \tag{10}$$

For the model, a micro-beam with two piezoelectric layers bonded through the entire of its upper and lower surfaces, total moment M_{tot} will be in the following form:

$$M_{tot} = M_{piezo} + M_{elastic} \tag{11}$$

where M_{piezo} relates to the bonded piezoelectric layers moment and $M_{elastic}$ relates to the elastic layer moment and can be obtained as following respectively:

$$\begin{aligned} M_{piezo} &= \int_{\frac{h}{2}}^{\frac{h}{2}+h_s} z\left(-zc_{11,2-D}\frac{\partial^2 w}{\partial x^2} + e_{31,2-D}\frac{\partial \phi}{\partial z}\right)bdz \\ &+\int_{-\frac{h}{2}-h_s}^{-\frac{h}{2}} z\left(-zc_{11,2-D}\frac{\partial^2 w}{\partial x^2} + e_{31,2-D}\frac{\partial \phi}{\partial z}\right)bdz = -E_p I_p \frac{\partial^2 w}{\partial x^2} + \frac{4be_{31,2-D}h_p}{\pi}\phi_p(x,t) \end{aligned} \tag{12}$$

$$M_{elastic} = \int_{-\frac{h}{2}}^{\frac{h}{2}} -E_e z^2 \frac{\partial^2 w}{\partial x^2} bdz \tag{13}$$

The same (same value and same polarization) external voltages applied to the piezoelectric layers cause to induce an axial tensile or compressive force along the length of the beam as following Eq. (14).

$$\begin{aligned} T_p &= \int_{\frac{h}{2}}^{\frac{h}{2}+h_s}\left(-zc_{11,2-D}\frac{\partial^2 w}{\partial x^2} + e_{31,2-D}\frac{\partial \phi}{\partial z}\right)bdz \\ &+\int_{-\frac{h}{2}-h_s}^{-\frac{h}{2}}\left(-zc_{11,2-D}\frac{\partial^2 w}{\partial x^2} + e_{31,2-D}\frac{\partial \phi}{\partial z}\right)bdz = 2e_{31,2-D}b\phi_a(t) = -2e_{31,2-D}bV_p \end{aligned} \tag{14}$$

According to Euler-Bernoulli beam theory and Eqs. (11) and (14), the nonlinear equation governing the micro-beam dynamic motion [18] will be as:

$$\begin{aligned} &\mu\frac{\partial^4 w(x,t)}{\partial x^4} - \frac{4be_{31,2-D}h_p}{\pi}\frac{\partial^2 \phi_p(x,t)}{\partial x^2} - (T_p + T_r)\frac{\partial^2 w(x,t)}{\partial x^2} + (\rho bh)_{eq}\frac{\partial^2 w(x,t)}{\partial t^2} \\ &+C\frac{\partial w(x,t)}{\partial t} = \mathrm{P}(V,w) = \frac{\varepsilon_o bV^2}{2(g_o - w)^2} \end{aligned} \tag{15}$$

where $\mu = \tilde{E}_e I_e + c_{11,2D} I_p$, $(\rho bh)_{eq} = (\rho_p b_p h_p) + (\rho_e b_e h_e)$. T_r is the axial residual stress of the beam. $\mathrm{P}(V,w)$ is the electrostatic pressure, ε_o is the dielectric coefficient of air, C is the micro-beam damping. I_p and I_e are respectively, moment of inertia of the piezoelectric layers and elastic layer. $\tilde{E}_e$ is the effective modulus of elasticity of the elastic layer. As the free charge density ρ_f inside the piezoelectric layer is zero, the electrostatic Maxwell's charge equilibrium equation can be written as following [27]:

$$\frac{\partial D_3}{\partial z} = \rho_f = 0 \tag{16}$$

With substitution of D_3, ε_x and E_3 from Eq. (5), Eq. (1) and Eq. (10) into Eq. (16) respectively, Eq. (17) and consequently Eq. (18) are obtained.

$$\frac{\partial\left(e_{31,2-D}\varepsilon_x + \varepsilon^{\varepsilon}_{3,2-D}E_3\right)}{\partial z} = 0 \tag{17}$$

$$e_{31,2-D}\frac{\partial^2 w(x,t)}{\partial x^2} + \varepsilon^{\varepsilon}_{3,2-D}\left(\frac{\pi}{h_p}\right)^2 \cos\left(\frac{\pi z_1}{h_p}\right)\phi_p(x,t) = 0 \tag{18}$$

Applying Galerkin based weighted residual method and integrating the Maxwell electricity equation (Eq. (18)) through the thickness of the piezoelectric layers in Eq. (19) leads to Eq. (20):

$$\int_{-\frac{h_p}{2}}^{\frac{h_p}{2}} \cos\left(\frac{\pi z_1}{h_p}\right)\left(e_{31,2-D}\frac{\partial^2 w(x,t)}{\partial x^2} + \varepsilon^{\varepsilon}_{3,2-D}\left(\frac{\pi}{h_p}\right)^2 \cos\left(\frac{\pi z_1}{h_p}\right)\phi_p(x,t)\right) dz_1 = 0 \tag{19}$$

$$\frac{2h_p e_{31,2-D}}{\pi}\frac{\partial^2 w(x,t)}{\partial x^2} + \varepsilon^{\varepsilon}_{3,2-D}\frac{\pi^2}{2h_p}\phi_p(x,t) = 0 \tag{20}$$

For convenience Eq. (20) can be rewritten as following:

$$\frac{\partial^2 \phi_p(x,t)}{\partial x^2} = -\frac{4{h_p}^2 e_{31,2-D}}{\varepsilon^{\varepsilon}_{3,2-D}\pi^3}\frac{\partial^4 w(x,t)}{\partial x^4} \tag{21}$$

Substituting Eq. (21) into Eq. (15) the governing equation of the beam motion can be written in the following form:

$$\left(\mu + \frac{16b\left(e_{31,2-D}\right)^2 {h_p}^3}{\varepsilon^{\varepsilon}_{3,2-D}\pi^4}\right)\frac{\partial^4 w(x,t)}{\partial x^4} - \left(T_p + T_r\right)\frac{\partial^2 w(x,t)}{\partial x^2} + (\rho bt)\frac{\partial^2 w(x,t)}{\partial t^2} + C\frac{\partial w(x,t)}{\partial t} = \frac{\varepsilon_o b V^2}{2\left(g_o - w\right)^2} \tag{22}$$

As shown the coupled equations of the beam dynamic motion and Maxwell electricity distribution are reduced to Eq. (22) and the effects of the applied voltage and piezoelectric layers is seen in the equivalent beam rigidity and tension.

3 SOLUTION

As clear, due to the existence of the strong nonlinear electrostatic force in the governing equation suggesting an analytical solution is impractical. Some researchers suggested linearization methods. But as the value of w with respect to the initial gap is considerable linearizing the electrostatic force about un-deflected position of the micro-beam will cause a significant error. To reduce this error here step by step linearizing the strong nonlinear electrostatic force is used to change the non-linear governing equation into a linear one [28]. This logic causes to solve some linearized equations sequentially instead of solving the non-linear equation.

Consider w^i is the deflection due to the applied voltage V^i. With increasing the applied voltage at $(i+1)th$ step as δV with respect to $(i)th$ step; the deflection will be increased as $\delta w = \psi$ like following:

$$V^{i+1} = V^i + \delta V \Rightarrow w^{i+1} = w^i + \delta w = w^i + \psi \tag{23}$$

So for step (i) we substitute V^i and w^i into the governing statically actuated beam we have:

$$\left(\mu + \frac{16b\left(e_{31,2-D}\right)^2 {h_p}^3}{\varepsilon^{\varepsilon}_{3,2-D}\pi^4}\right)\frac{\partial^4 w^i}{\partial x^4} - \left(T_p + T_r\right)\frac{\partial^2 w^i}{\partial x^2} = \frac{\varepsilon_o b V^{i2}}{2\left(g_o - w\right)^2} \tag{24}$$

Then at step $(i+1)$ we have:

$$\left(\mu + \frac{16b\left(e_{31,2-D}\right)^2 {h_p}^3}{\varepsilon^{\varepsilon}_{3,2-D}\pi^4}\right)\left(\frac{\partial^4 w^i}{\partial x^4} + \frac{\partial^4 \psi}{\partial x^4}\right) - \left(T_p + T_r\right)\left(\frac{\partial^2 w^i}{\partial x^2} + \frac{\partial^2 \psi}{\partial x^2}\right)$$
$$= \frac{\varepsilon_o b V^{i2}}{2\left(g_o - w\right)^2} + \frac{\varepsilon_o b V^i \delta V}{\left(g_o - w\right)^2} + \frac{\varepsilon_o b V^{i2} \psi}{\left(g_o - w\right)^3} \tag{25}$$

In right side of Eq. (25) electrostatic loading is expanded by means of Taylor series to make analytical possible. In order to obtain governing equation to find at the subsequent steps; with comparison of $(i+1)th$ step and $(i)th$ step equations we have:

$$\left(\mu + \frac{16b\left(e_{31,2-D}\right)^2 {h_p}^3}{\varepsilon^{\varepsilon}_{3,2-D}\pi^4}\right)\frac{\partial^4 \psi}{\partial x^4} - \left(T_p + T_r\right)\frac{\partial^2 \psi}{\partial x^2} = \frac{\varepsilon_o b V^i \delta V}{\left(g_o - w\right)^2} + \frac{\varepsilon_o b V^{i2} \psi}{\left(g_o - w\right)^3} \tag{26}$$

Obtained linear equation, presents the micro-beam deflection due to increasing the applied voltage as δV. The micro-beam deflection can be assumed as a combination of a complete set of linearly independent shape functions as following [29]:

$$\psi = \sum_{i=1}^{n} a_i \varphi_i\left(x\right) \tag{27}$$

where φ_i is the shape function, and a_i is the unknown coefficients of shape function, n shows the number of shape functions used to find ψ with an acceptable accuracy. By substituting Eq. (27) into the Eq. (26), micro-beam deflection equation will be as:

$$\sum_{i=1}^{n} a_i \left(\mu + \frac{16b\left(e_{31,2-D}\right)^2 {h_p}^3}{\varepsilon^{\varepsilon}_{3,2-D}\pi^4} \right) \frac{\partial^4 \varphi_i}{\partial x^4} - \sum_{i=1}^{n} a_i \left(T_p + T_r\right) \frac{\partial^2 \varphi_i}{\partial x^2} - \sum_{i=1}^{n} a_i \frac{\varepsilon_o b V^2 \varphi_i}{\left(g_o - w\right)^3} - \frac{\varepsilon_o b V \delta V}{\left(g_o - w\right)^2} = R(x) \tag{28}$$

where $R(x)$ is some residuals, due to the finite number of used shape functions. The obtained equation can be solved by using Galerkin based weighted residual method [21], thus:

$$\int_0^L \varphi_j R(x) dx = 0 \qquad j = 1,...,n \tag{29}$$

Then by substituting Eq. (28) into Eq. (29) as:

$$\begin{aligned} &\sum_{i=1}^{n} a_i \int_0^L \varphi_j \left(\mu + \frac{16b\left(e_{31,2-D}\right)^2 {h_p}^3}{\varepsilon^{\varepsilon}_{3,2-D}\pi^4} \right) \frac{\partial^4 \varphi_i}{\partial x^4} dx - \sum_{i=1}^{n} a_i \int_0^L \left(T_p + T_r\right) \varphi_j \frac{\partial^2 \varphi_i}{\partial x^2} dx \\ &- \sum_{i=1}^{n} a_i \int_0^L \frac{\varepsilon_o b V^2 \varphi_i}{\left(g_o - w\right)^3} \varphi_j \, dx = \int_0^L \frac{\varepsilon_o b V \delta V}{\left(g_o - w\right)^2} \varphi_j \, dx, \qquad j = 1,...,n \end{aligned} \tag{30}$$

This equation can be reduced into following form:

$$\left[\mathbf{K}^m - \mathbf{K}^T - \mathbf{K}^e\right]_{n*n} \left[\boldsymbol{a}\right]_{n*1} = \left[\boldsymbol{F}^e\right]_{n*1} \tag{31}$$

Finally the elements of the stiffness and force matrices can be written in the following form:

$$\begin{aligned} &K^m_{ij} = \int_0^L \varphi_j \left(\mu + \frac{16b\left(e_{31,2-D}\right)^2 {h_p}^3}{\varepsilon^{\varepsilon}_{3,2-D}\pi^4} \right) \frac{\partial^4 \varphi_i}{\partial x^4} dx \; ; \quad K^T_{ij} = \int_0^L \left(T_p + T_r\right) \varphi_j \frac{\partial^2 \varphi_i}{\partial x^2} dx \\ &K^e_{ij} = \int_0^L \frac{\varepsilon_o b V^2 \varphi_i}{\left(g_o - w\right)^3} \varphi_j \, dx \; ; \qquad F^e_j = \int_0^L \frac{\varepsilon_o b V \delta V}{\left(g_o - w\right)^2} \varphi_j \, dx \end{aligned} \tag{32}$$

4 NUMERICAL RESULTS

Consider, PZT-4 as the piezoelectric layers, which are bonded to the upper and lower side of the silicon micro-beam with original mechanical and electrical properties, and geometrical dimensions as listed in Table 1. [30].

Let us to control the pull-in voltage; which is occurred due to the application of the electrostatic voltage, by applying different piezoelectric voltages to the piezoelectric layers. Here thickness ratio r_p is defined as the ratio of the piezoelectric layer thickness respect to the elastic layer thickness. The proposed model numerical results of pull-in voltage for different thickness ratios are investigated, and compared with the results of the model expressed by Crawley and Lius et al. [31]. As shown in Table 2 . applying positive piezoelectric voltage decreases pull-in voltage. In fact the positive piezoelectric voltage causes a compressive stress and reduces the equivalent mechanical stiffness of the micro-beam. And inversely applying negative piezoelectric voltage causes a tensile stress in the micro-beam and stiffens the micro-beam and consequently increases the Pull-in voltage. Importance of the pull-in voltage control becomes significant, where the pull-in voltage is a design restriction. For example in MEMS switches the value of the supplied voltage is restricted to $3-5$ (volt), where for the micro-beams used in MEMS switches the pull-in voltage usually is about 25 (volt) that is undesirable. One of the methods to overcome this problem is, use of piezoelectric layers bonded to the upper and lower sides of the micro-beam surfaces. By applying a proper voltage to the piezoelectric layers the pull-in voltage can be decreased down to an acceptable value.

Table 1
Geometrical and material properties of the silicon micro-beam and piezoelectric layers [30]

	Micro-beam	Piezoelectric Layer
Length	$350\mu m$	$350\mu m$
Width	$50\mu m$	$50\mu m$
Young's modulus	$169GPa$	
Poisson's ratio	0.06	0.3
Mass density	$2,231Kg/m^3$	$7,500Kg/m^3$
e_{31}	-	-5.2
e_{33}	-	15.1
c_{11}	-	$13.9GPa$
c_{12}	-	$7.78GPa$
c_{33}	-	$11.743GPa$
c_{13}	-	$7.428GPa$
$\varepsilon_3^{\varepsilon}$	-	$5.62\times10^{-9}\,F/m$
$\varepsilon_1^{\varepsilon}$	-	$6.46\times10^{-9}\,F/m$
g_o	$1\mu m$	
ε_o	$8.85418710^{-12}\,F/m$	

In Table 2 . are given the values of the calculated pull-in voltages for the fixed-fixed electrostatic actuator for different thickness ratios and different voltages applied to the piezoelectric layers and are compared to those obtained by Crawley and Lius et al. model. As shown in Table 2 . for small thickness ratios like $r_p = 0.1$ the results of the proposed model for all piezoelectric voltages are equal with the obtained results of Crawley and Lius et al. [31] model, but by increasing the thickness ratio, the difference between the results of two models increases, especially for the positive voltages applied to the piezoelectric layers.

Commonly, residual stresses play an important role in fixed-fixed micro-beams analysis, which may happen due to thermal mismatch effects in micro-beams production process. Somehow, it can be as a controlling parameter to change the micro-beam stiffness, consequently pull-in voltage, or frequency.

In Fig. 2 the obtained pull-in voltages for a clamped-clamped micro-beam with elastic layer thickness $h = 1\mu m$, and thickness ratio $r_p = 1.5$ for different residual stresses are shown. Here as it appears in Fig. 2 by applying different voltages to the bonded piezoelectric layers, desirable or undesirable effects of the residual stress can be measured or controlled. As obvious from Fig. 2 different piezoelectric voltages can be applied to tune the micro-beam stiffness by eliminating adverse effects of the existing residual stresses, and or successively intensify its suitable effects.

Table 2
The values of the calculated pull-in voltages for the fixed-fixed electrostatic actuator for different piezoelectric voltage

Piezoelectric voltage		-2.5 volt	0 volt	2.5 volt	5 volt	7.5 volt	15 volt
$r_p = .1$ $h = 3\mu m$	Proposed	28.24	23.74	18.05	9.07		
	Crawley & Lius	28.23	23.74	18.05	9.07		
Δ_1		0.03 %	0 %	0 %	0 %		
$r_p = 1$ $h = 1.5\mu m$	Proposed	31.84	27.93	23.3	17.38	7.51	
	Crawley & Lius	31.58	27.63	22.94	16.88	6.25	
Δ_2		0.95 %	1.1%	1.5%	2.96%	20.16 %	
$r_p = 2.5$ $h = 1\mu m$	Proposed	45.53	42.87	40.02	36.94	32.55	19.94
	Crawley & Lius	44.66	41.95	39.04	35.87	32.36	17.84
Δ_3		1.9 %	2.2 %	2.5%	2.9 %	3.67 %	11.77 %

With: $\Delta_i(\%) = \dfrac{(obtained\ result - crawley\ model\ results)}{crawley\ model\ results} * 100$

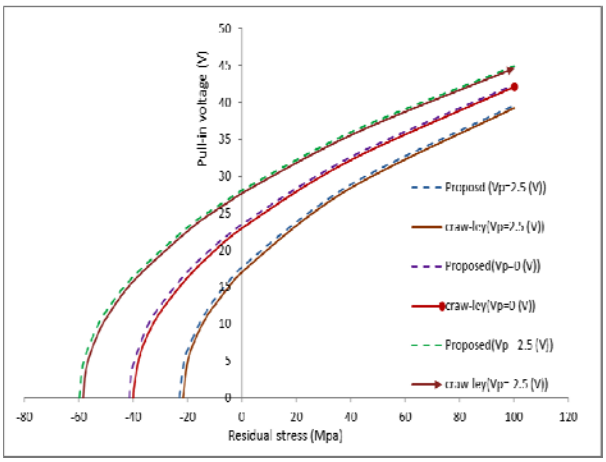

Fig.2
The Pull-in voltage versus residual stress (MPa) for different piezoelectric voltages.

As shown in the governing Eq. (23), electric potential distribution affects the stiffness of the micro-beam; furthermore modulus of elasticity and moment of inertia. The electric potential distribution effect on the stiffness of the micro-beam, by increasing the thickness ratio becomes considerable. In Fig. 3 the obtained results for the pull-in voltage of the present model are compared to the results of the model expressed by Crawley and Lius et al. [31], for different thickness ratios (r_p) for the cases with and without voltage applied to the piezoelectric layers. As shown the results of the both models for $r_p \ll 1$ approximately are same, but as r_p increases, the difference between the results of the models becomes visible.

In Fig.4 for different residual stresses, the effect of the thickness ratio r_p on the micro-beam stiffness and pull-in voltage is investigated. The effect of the electric potential distribution on the pull-in voltage becomes more significant as r_p increases, which causes to large difference between both models in the estimation of the pull-in voltage. This fact requires the necessity of considering the proposed model for large piezoelectric thickness ratio.

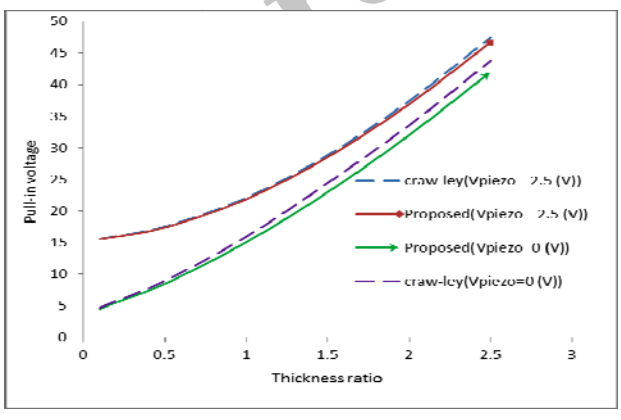

Fig.3
The pull-in voltage versus the thickness ratio for different piezoelectric voltages.

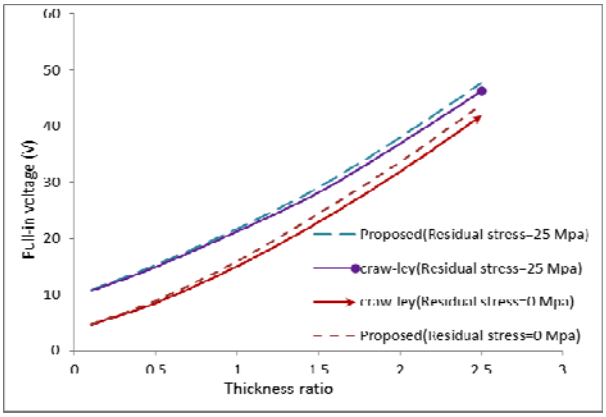

Fig.4
The pull-in voltage versus the thickness ratio for different residual stresses.

4 CONCLUSIONS

Mechanical behavior of a fixed-fixed micro-beam, bonded with two piezoelectric layers through its upper and lower surfaces was studied, which undergoes both electrostatic and piezoelectric actuations. The non-linear governing equation of the micro-beam based on Euler-Bernoulli beam theory involving with the two dimensional electric potential distribution in the piezoelectric layers was derived. The results showed that the electric potential distribution causes to increase the micro-beam stiffness. The micro-beam stiffening depends on the piezoelectric layer thickness to the elastic layer thickness. The obtained results of the proposed model were compared with the expressed model by Crawley and Lius. And it was shown that, by increasing the thickness ratio, the differences between the results of the proposed model and those existing in literature, become more considerable. So in these cases the effect of the electric potential distribution on the mechanical behavior should be considered.

REFERENCES

[1] Fathalilou M., Motallebi A., Yagubizade H., Rezazadeh G., Shirazi K., Alizadeh Y., 2009, Mechanical Behavior of an Electrostatically-Actuated Micro-beam under Mechanical Shock, *Journal of Solid Mechanics* **1**: 45-57.

[2] Yao J.J., 2000, RF-MEMS from a device perspective, *Journal of Micromechanics and Micro engineering* **10**: 9-38.

[3] Afrang S., Abbaspour E., 2002, A low voltage electrostatic torsional micro machined microwave actuator, *In: Proceedings of the 2002 IEEE international conference on semiconductor electronics (ICSE 2002) Penang*, Malaysia 100–104.

[4] Balaraman D., Bhattacharya S.K., 2002, Low-cost low actuation voltage copper RF MEMS actuators. *In: Proceeding of the Microwave Symposium Digest, 2002 IEEE MTT-S International, Seattle, WA* **2**: 1225–1228.

[5] Peroulis D., Pacheo S.P., Sarabandi K., 2003, Electromechanical considerations in developing low-voltage RF MEMS actuators, *IEEE Transaction on microwave theory and thecniques* **51**(1): 259–270.

[6] Sbaizero O., Lucchini E., 1996, Influence of residual stresses on the mechanical properties of a layered ceramic composite, *Journal of the European Ceramic Society* **16**(8): 813-818.

[7] Pascual J., Lube T., Danzer R., 2008, Fracture statistics of ceramic laminates strengthened by compressive residual stresses, *Journal of the European Ceramic Society* **28**(8): 1551-1556.

[8] Hayes M., Rivlin R.S., 1961, Surface waves in deformed elastic materials, *Archive for Rational Mechanics and Analysis* **8**: 359–439.

[9] Hirao M., Fukuoka H., Hori K., 1981, Acoustoelastic effect of Rayleigh surface wave in isotropic material, *Journal of Applied Mechanics* **48**: 119–43.

[10] Kumar A., Weizel U., Mittemeijer E.J., 2006, Analysis of gradients of mechanical stresses by X-ray diffraction measurements at fixed penetration/information depths, *Journal of Applied Crystallography* **39**: 633-646**.**

[11] Cammarata R.C., Sieradzki, K., Spaepen, F., 2000, Simple model for interface stresses with application to misfit dislocation generation in epitaxial thin films, *Journal of Applied Physics* **87**(3): 1227-1234.

[12] Freund L.B., Suresh S., 2003, Thin Film Materials: Stress, Defect Formation and Surface Evolution, *Cambridge University Press*.

[13] Quang H.L., He Q.C., 2009, Estimation of the effective thermo-elastic moduli of fibrous nano composites with cylindrically anisotropic phases, *Archive for Applied Mechanics* **79**: 225–248.

[14] Hosseinzadeh A., Ahmadian M.T., 2010, Application of Piezoelectric and Functionally Graded Materials in Designing Electrostatically Actuated Micro Switches, *Journal of Solid Mechanics* **2**: 179-189.
[15] Coughlin M.F., Stamenovic D., Smits J.G., 1996, Determining material stiffness using piezoelectric bimorphs, in: *Proceedings of the 1996 IEEE ultrasonic Symposium* **2**: 1607–1610.
[16] Mortet V., Petersen R., Haenen K., Olieslaeger M. D., 2006, Wide range pressure sensor based on a piezoelectric bimorph micro-cantilever, *Applied Physic Letters* **88** (13) : 133511–15.
[17] Olli K., Kruusing A., Pudas M., Rahkonen T., 2009, Piezoelectric bimorph charge mode force sensor. *Journal of Sensors and Actuators A: Physical* **153**: 42–49.
[18] Rezazadeh G., Tahmasebi A., Zubstov M., 2006, Application of piezoelectric layers in electrostatic MEM actuators: controlling of pull-in voltage, *Microsystem Technologies* **12**: 1163–1170.
[19] Zamanian M., Khadem S.E., Mahmoodi S.N., 2008 , The effect of a piezoelectric layer on the mechanical behavior of an electrostatic actuated micro-beam, *Smart Materials and Structures* **17** : 065024–15.
[20] Rezazadeh G., Tahmasebi A., 2009, Electromechanical behavior of micro-beams with piezoelectric and electrostatic actuation, *Sensing and Imaging: an International Journal* **10**: 15–30.
[21] Rezazadeh G., Fathalilou M., Shabani R., 2009, Static and dynamic stabilities of a microbeam actuated by a piezoelectric voltage, *Microsystem Technologies* **15**: 1785–1791.
[22] Azizi S., Rezazadeh G., Ghazavi M.R., Esmaeilzadeh Khadem S.,2012, Parametric excitation of a piezoelectrically actuated system near Hopf bifurcation, *Journal of Applied Mathematical Modelling* **36** : 1529–1549.
[23] Quek S.T., Wang Q., 2000, On dispersion relations in piezoelectric coupled plate Structures, *Smart Material Structure* **9**: 859–67.
[24] Moheimani R., Fleming A.J., 2006, Piezoelectric Transducers for Vibration Control and Damping (Advances in Industrial Control), First Edition, *Springer*.
[25] Zhu M., Leighton G., 2008, Dimensional Reduction Study of Piezoelectric Ceramics Constitutive Equations from 3-D to 2-D and 1-D, *IEEE Transactions on Ultrasonics, Ferroelectrics, and Frequency Control* **55**(11): 2377-2383.
[26] Pietrzakowski M., 2007, Piezoelectric control of composite plate vibration: Effect of electric potential distribution, *Computers and Structures* **86**: 948–954.
[27] Kant T., Shiyekar S.M., 2008, Cylindrical bending of piezoelectric laminates with a higher order shear and normal deformation theory, *Computers and Structures* **86** : 1594–1603.
[28] Nabian A., Rezazadeh G., Haddad-derafshi M., Tahmasebi A., 2008, Mechanical behavior of a circular micro plate subjected to uniform hydrostatic and non-uniform electrostatic pressure, *Microsystem Technologies* **14**: 235–240.
[29] Nayfeh A.H., Mook D.T., 1979, Nonlinear oscillations. Wiley, NewYork, *Microsystem Technologies* **14**: 235–240.
[30] Ramamurty U., Sridhar S., Giannakopolos A. E., Suresh S., 1999, An experimental study of spherical indentation on piezoelectric materials, *Acta material* **47**(8): 2417-2430.
[31] Crawley E. F., Luis J. D., 1987, Use of piezoelectric actuators as elements of intelligent structures, *AIAA Journal* **25**(10): 1373–1385.